J|A|C|S
ARTICLES
Published on Web 11/24/2005

RNA-Mediated Control of Metal Nanoparticle Shape

Lina A. Gugliotti,[†] Daniel L. Feldheim,*[,†] and Bruce E. Eaton*[,†,‡]

Contribution from the W. M. Keck Center for RNA-Mediated Materials Synthesis, Department of Chemistry, North Carolina State University, Raleigh, North Carolina 27695

Received July 26, 2005; E-mail: Dan_Feldheim@NCSU; Bruce.Eaton@colorado.edu

Abstract: RNA sequences previously isolated by in vitro selection were further characterized for their ability to control palladium particle growth. Five pyridyl-modified RNA sequences (Pdases) representing each of the different evolved families were found to form hexagonal plates with a high degree of shape specificity. However, a sixth nonrelated pyridyl-modified RNA sequence was found to form exclusively cubic particles under identical conditions. Replacing pyridyl-modified RNA with native RNA resulted in a complete loss of RNA function. Removing the 3′-fixed sequence region from the Pdase had little effect on particle growth; however, further truncations into the variable region resulted in a significant loss of activity and particle shape control. These Pdases were selected using the organometallic precursor complex tris(dibenzylideneacetone) dipalladium(0) ($[Pd_2(DBA)_3]$). Changing the metal center and ligand of the group VIII organometallic precursor complex revealed a strong dependence of particle growth and shape on the DBA ligands. Changing the metal center from Pd to Pt while retaining the DBA ligands gave predominantly hexagonal Pt, but with a decrease in shape control. Taken together, the results of this study suggest that the full-length Pdases contain active sites capable of highly specific molecular recognition of organometallic complexes as particle formation reagents.

Introduction

The size, shape, and crystal structure of a solid-state material can have a profound impact on its chemical and physical properties. The optical properties and catalytic activities of metals,[1,2] the magnetic moments of metal oxides,[3] and the electron transport characteristics of semiconductors,[4] for example, all change dramatically with crystal size, polymorph, and macroscopic morphology. Despite the importance of controlling crystal morphology, modern crystal engineering remains largely an empirical discipline with few exceptions. Crystal size and shape are typically manipulated by controlling growth kinetics. This can be accomplished by adjusting monomer concentration and temperature and by adding small molecules, surfactants, or polymeric capping reagents.[5−7] While the molecular-level interactions between capping reagents and a growing crystal are currently unknown for many systems, it is generally postulated that an additive binds to the crystal in a face-selective fashion. This can slow the growth of that face relative to other growth directions, resulting in highly anisotropic crystal shapes.[8] Choosing the correct additive is crucial and largely a trial-and-error process. If the binding interactions between the capping reagent and a crystal are too strong, only very small crystal nuclei will form. If they are too weak, face-selective growth will not occur.

Nature has provided some of the best examples of selective materials crystal growth. In an attempt to emulate these controlled growth processes, crystal engineering research has recently been directed toward understanding how biological systems create the breadth of sophisticated material architectures found in nature. Nearly every living organism on earth synthesizes a solid-state material, some for structural integrity or protection, others for biosphere function such as light focusing[9] or magnetotaxis.[10] Many of these functions have now been mimicked effectively in the lab; proteins, peptides, and ampiphilic monolayers that closely resemble nature's ability to form materials have been isolated. Biomimetic methods have been used to prepare oriented hydroxyapatite crystals similar to human bone, silica fibrils reminiscent of marine sponges, and porous calcium carbonate networks such as those found in marine brittlestars.[11−13] These methods have been extended to the formation of other materials not found in nature such as

[†] North Carolina State University.
[‡] Current address: Department of Chemistry and Biochemistry, University of Colorado, Boulder, CO 80309.

(1) Tam, F.; Moran, C.; Halas, N. *J. Phys. Chem. B* **2004**, *108*, 17290−17294.
(2) Jin, R.; Cao, Y.; Mirkin, C. A.; Kelly, K.; Schatz, G.; Zheng, J. *Science* **2001**, *294*, 1901−1903.
(3) Liu, C.; Zhang, Z. J. *Chem. Mater.* **2001**, *13*, 2092−2096.
(4) Huynh, W. U.; Dittmer, J. J.; Alivisatos, A. P. *Science* **2002**, *295*, 2425−2427.
(5) Kirkland, A. I.; Jefferson, D. A.; Duff, D. G.; Edwards, P. P.; Gameson, I.; Johnson, B. F. G.; Smith, D. J. *Proc. R. Soc. London, Ser. A* **1993**, *440*, 589−609.
(6) Busbee, B. D.; Obare, S. O.; Murphy, C. J. *Adv. Mater.* **2003**, *15*, 414−416.
(7) Ahmadi, T. S.; Wang, Z. L.; Henglein, A.; El-Sayed, M. A. *Chem. Mater.* **1996**, *8*, 1161−1164.
(8) Puntes, V. F.; Krishnan, K.; Alivisatos, A. P. *Top. Catal.* **2002**, *19*, 145−148.
(9) Vukusic, P.; Sambles, J. R. *Nature* **2003**, *424*, 852−855.
(10) Matsunaga, T.; Okamura, Y. *Trends Microbiol.* **2003**, *11*, 536−541.
(11) Aizenberg, J.; Muller, D. A.; Grazul, J. L.; Hamann, D. R. *Science* **2003**, *299*, 1205−1208.
(12) Cha, J. N.; Shimizu, K.; Zhou, Y.; Christiansen, S. C.; Chmelka, B. F.; Stucky, G. D.; Morse, D. E. *Proc. Natl. Acad. Sci. U.S.A.* **1999**, *96*, 361−365.
(13) Hartgerink, J. D.; Beniash, E.; Stupp, S. I. *Science* **2001**, *294*, 1684−1688.

10.1021/ja055039o CCC: $30.25

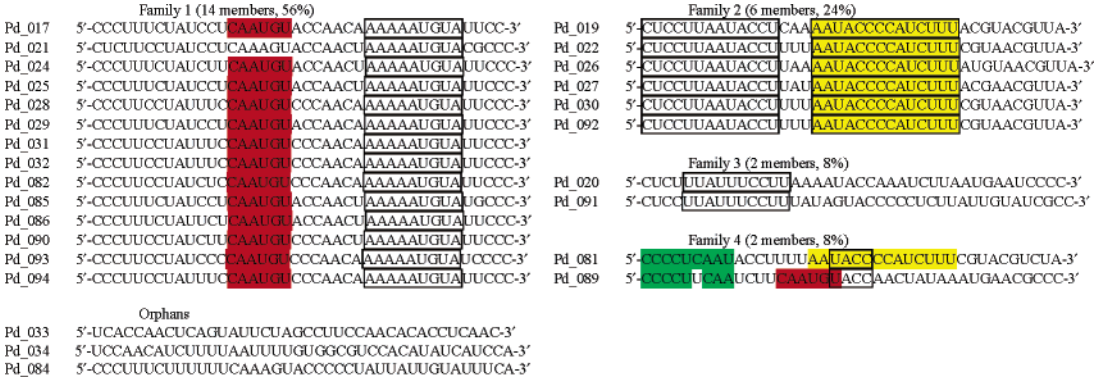

Figure 1. Evolved RNA sequences capable of catalyzing the formation of hexagonal Pd platelets. The sequences are grouped into families related by highly conserved regions (shown in color).

metallized DNA wires[14] and viral-templated liquid crystals.[15] Many of these biomimetic syntheses utilize protein or peptide fragments. Given recent developments in RNA catalysis, it was of interest to determine if selected sequences[16] of this highly structured biopolymer could also control materials crystal growth.

A new approach to the discovery of unique RNA sequences that can catalyze crystal growth and direct crystal shape was demonstrated recently in our labs.[16] In that work, modified (4-pyridyl-uridine) RNA libraries[17,18] were used and in vitro selection based on particle size was performed until a small subset of sequences was found that catalyzed the formation of thin (ca. 20 nm) hexagonal palladium plates from the zerovalent metal complex precursor tris(dibenzylideneacetone) dipalladium-(0) ($[Pd_2(DBA)_3]$). RNA in vitro selection[19−25] has a number of attributes as an alternative materials synthesis tool. A large number of sequences and crystals can be screened simultaneously and selected for a desired size or shape. In addition, RNA-mediated evolution is performed in a cyclic process, multiple times until the selected property emerges. During this cyclic process, mutations can occur that alter the interactions between a pool of RNA sequences and their concomitant growing crystal. When successful, this materials evolution process ultimately converges on RNA structures that reproducibly fold into intricate 3D structures dictated by their sequence. This leads to the questions we pose herein: Do all evolved sequences in a given family (Figure 1) yield the same particle shape? Is the metal, ligand, or both important in the growth process, or is the particle shape controlled exclusively by the folded RNA acting as a template? Is the entire RNA molecule required or will truncated sequences maintain activity toward particle shape control? Is the pyridyl-modified uridine used to discover the active RNA sequences required, or can native uridine be used in its place?

Results

The RNA in vitro selection that gave the sequences capable of synthesizing hexagonal Pd particles (Pdases) was previously reported.[16] It began with a chemically synthesized library of 10^{14} unique ssDNA sequences, 87 bp in length, containing a center region of 40 bp, random in sequence.[16] Two-cycle PCR was used to convert the ssDNA library into dsDNA, and T7 RNA polymerase was used to transcribe the dsDNA library into an ssRNA library containing ca. 10^{14} sequences. During transcription, 5-(4-pyridylmethyl)-UTP was incorporated into the RNA to provide additional metal coordination sites augmenting the heterocyclic nitrogens present in native RNA. The RNA library was incubated for 2 h at ambient temperature with $[Pd_2(DBA)_3]$. For selection, RNA sequences were required either to mediate the formation of Pd metal particles and remain bound to those particles or simply to bind to particles formed spontaneously or by other RNA sequences. Size exclusion membranes (100 kD cutoff) and native polyacrylamide gel (6%) electrophoresis gel mobility shift-dependent partitioning were used to select for particles that were formed in the presence of RNA. The selected RNA was reverse-transcribed to give a cDNA copy of the "winning" RNA sequences. RNA sequences that did not form or bind to particles in each selection cycle were discarded. Finally, the evolved RNA pool was cloned and sequenced, and the active Pdase RNA sequences were grouped into families related by conserved regions (Figure 1).

Sequence-Dependent Pd Particle Growth. From Figure 1 it is clear that the selection converged on highly conserved sequences. It was of interest to determine if all of these sequences in fact assembled the same shape and size Pd particle. However, significant sequence variability was found outside the conserved sequence region, and this portion of the molecule might play an important role in dictating crystal growth and shape. When representative sequences from each respective family were incubated with $[Pd_2(DBA)_3]$ individually (isolates 17, 19, 20, 81, and 84), each was found to yield hexagonal Pd plates exclusively, consistent with crystal shape being correlated with the conserved sequence motif (Figure 2A). In contrast to the RNA Pdases of the sequences families, orphan sequence Pdase 34 yielded exclusively Pd cubes (Figure 2B). The average size ($w \times l$) of cubic particles formed in 2 h was 0.10 μm ± 0.05 μm × 0.07 μm ± 0.02 μm. Multiple experiments gave

(14) Yan, H.; Park, S. H.; Finkelstein, G.; Reif, J. H.; Labean, T. H. *Science* **2003**, *301*, 1882−1884.
(15) Lee, S. W.; Lee, S. K.; Belcher, A. M. *Adv. Mater.* **2003**, *15*, 689−692.
(16) Gugliotti, L.; Feldheim, D. L.; Eaton, B. *Science* **2004**, *304*, 850−852.
(17) Dewey, T. M.; Zyzniewski, M. C.; Eaton, B. E. *Nucleosides Nucleotides* **1996**, *15*, 1611−1617.
(18) Vaught, J.; Dewey, T. M.; Eaton, B. *J. Am. Chem. Soc.* **2004**, *126*, 11231−11237.
(19) Eaton, B. E. *Curr. Opin. Chem. Biol.* **1997**, *1*, 10−16.
(20) Nieuwlandt, D.; West, M.; Cheng, X. Q.; Kirshenheuter, G.; Eaton, B. E. *ChemBioChem* **2003**, *4*, 651−654.
(21) Tarasow, T. M.; Tarasow, S. L.; Eaton, B. E. *J. Am. Chem. Soc.* **2000**, *122*, 1015−1021.
(22) Kuhne, H.; Joyce, G. F. *J. Mol. Evol.* **2003**, *57*, 292−298.
(23) Tuerk, C.; Gold, L. *Science* **1990**, *249*, 505−510.
(24) Ellington, A. D.; Szostak, J. W. *Nature* **1992**, *355*, 850−852.
(25) Eaton, B. E.; Holley, B. In *Evolutionary Methods in Biotechnology*; Brakmann, S., Schwienhorst, A., Eds.; Wiley-VCH: Weinheim, Germany, 2004; pp 87−111.

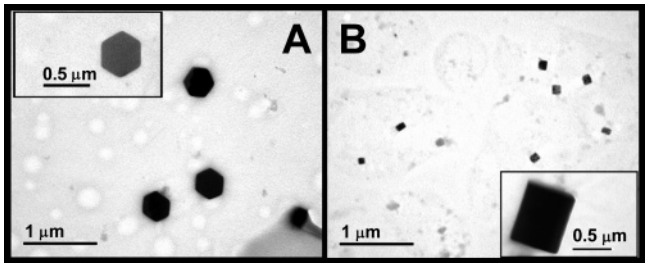

Figure 2. TEM micrographs of (A) hexagonal palladium particles formed in the presence of Pdase 17 and (B) cubic palladium particles formed in the presence of Pdase 34.

reproducible size distributions and exclusive shape control based on Pdase sequence. Thermal denaturation of Pdase 17 resulted in complete loss of shape control and a low yield of solid material consistent with the importance of folded RNA structure. It is now clear that RNA Pdases can control crystal shape, dictated by their sequence, and associated 3D structure.

It seemed reasonable that Pdase sequence families made related palladium particle shapes and that the conserved motif was essential in determining particle shape, but it was unclear what role the more variable parts of the sequence played. To investigate the importance of these more variable sequence regions on particle formation, two new truncated RNA sequences were enzymatically synthesized from chemically prepared DNA templates (Figure 3). In one sequence (truncate 1), the 3′-fixed region was removed from the full-length Pdase 17 template, leaving only the conserved sequence and variable portion. In the second sequence (truncate 2), the 3′-fixed region and four nucleotides of the variable region were removed from the original Pdase 17 template. Both truncates were subjected to the [$Pd_2(DBA)_3$] precursor under identical incubation and partitioning methods used in the selection (e.g., ambient temperature for 2 h), and the resulting material was analyzed by transmission electron microscopy (TEM). Both hexagonal and spherical particles were observed with truncate 1, while particles of undefined shape were observed with truncate 2. The estimated yield as determined by TEM of particles generated with truncates 1 and 2 was relatively poor in comparison with the full-length Pdase 17. These results suggest that the fixed region of the sequence must function in the structural context of the variable region in maintaining the required 3D structure for creating hexagonal Pd particles.

In the original selection experiments it was postulated that pyridyl modification could provide added diversity in Pd−ligand interactions and that expanding the chemical diversity of the RNA would be advantageous. However, it remained to be tested if in fact the pyridyl modification provided any benefit at all in these sequences. The importance of the pyridyl modification was examined by replacing pyridyl-modified UTP with native UTP for both Pdase 17 and 34 and investigating the particle formation for the resulting RNA molecules. In both cases, no

Table 1. Metal Precursor Effects on Particle Shape and Size

RNA isolate	metal precursor	particle shape	size (μm)	% population
17	$Pd_2(DBA)_3$	hexagonal	1.24 ± 0.57	100
	$Pt_2(DBA)_3$	spherical	0.10 ± 0.06	14
		cubic	0.22 ± 0.13	16
		hexagonal	0.46 ± 0.22	69
	$Pd(PPh_3)_4$	spherical	0.27 ± 0.16	100
	$Pt(PPh_3)_4$	spherical	0.007 ± 0.003	100
	$Ni(PPh_3)_4$	spherical	0.27 ± 0.10	100
34	$Pd_2(DBA)_3$	cubic	0.10 ± 0.05	100
	$Pt_2(DBA)_3$	spherical	0.16 ± 0.05	2
		cubic	0.14 ± 0.07	29
		hexagonal	0.37 ± 0.16	68
	$Pd(PPh_3)_4$	spherical	0.31 ± 0.29	100
	$Pt(PPh_3)_4$	spherical	0.009 ± 0.007	100
	$Ni(PPh_3)_4$	spherical	0.24 ± 0.10	100

examples of hexagonal or cubic Pd particles were observed and only a low yield of spherical particles was found by TEM. Knowing that the pyridyl group was important for Pdase activity and that this was a good ligand for Pd^0, it was of interest to determine how the Pd precursor ligands might influence particle growth.

Metal and Ligand Dependence. The RNA Pdase sequences showed rapid kinetics in particle growth (>1 μm in <1 min). An essential part of any Pd particle growth mechanism requires the elimination of ligands. This elimination process could occur by associative or dissociative processes where the RNA played a role in displacing ligands or stabilizing coordinatively unsaturated Pd intermediates. If Pd−ligand bonds were important, then studying other metal−ligand combinations in the group VIII triad (Ni, Pd, and Pt) as precursors for the Pdases might reveal differences in metal particle shape. It is well-known that metal−ligand bond strengths increase moving down this triad in the periodic table. It was of interest to determine if the Pdases were capable of discriminating different metal precursors, either Pd with different ligands or the transition metals of the same triad (Pt and Ni). The effects of changing the group VIII metal precursor on particle shape and size were studied with both isolates 17 and 34. Pyridyl-modified Pdases 17 and 34 (1 μM) were incubated in the presence of various metal precursors (400 μM) for 2 h at ambient temperature, and the resulting particles were examined by TEM. Focusing first on the results for Pdase 17, changing the metal center to Pt, while retaining the DBA ligands, resulted in a predominance of hexagonal Pt particles, but also a minor fraction of cubic and spherical particles (Figure 4, Table 1). Growth of hexagonal particles was 0.22 μm in 2 h compared to 1.24 μm ± 0.57 μm for the same sequence with [$Pd_2(DBA)_3$]. Changing the ligand to triphenylphosphine (PPh_3) resulted in the formation of spherical particles only, independent of the metal center (Pd, Pt, Ni). When [$Pt(PPh_3)_4$] was used as the precursor, particles only reached a size of ca. 7 nm, compared to >200 nm for all other precursors.

5′--23 Fixed--CCCUUUCUAUCCUCAAUGUACCAACAAAAAAUGUAUUCC---24 Fixed--3′

5′--23 Fixed—CCCUUUCUAUCCUCAAUGUACCAACAAAAAAUGUAUUCC--3′

5′--23 Fixed—CCCUUUCUAUCCUCAAUGUACCAACAAAAAAUGUA--3′

Figure 3. Full-length 87-mer Pdase 17 sequence (top) and the 3′-truncated sequences examined for the ability to catalyze the formation of Pd hexagons. Truncate 1 (middle) was a 62-mer, and truncate 2 (bottom) was a 58-mer. Conserved region is underlined.

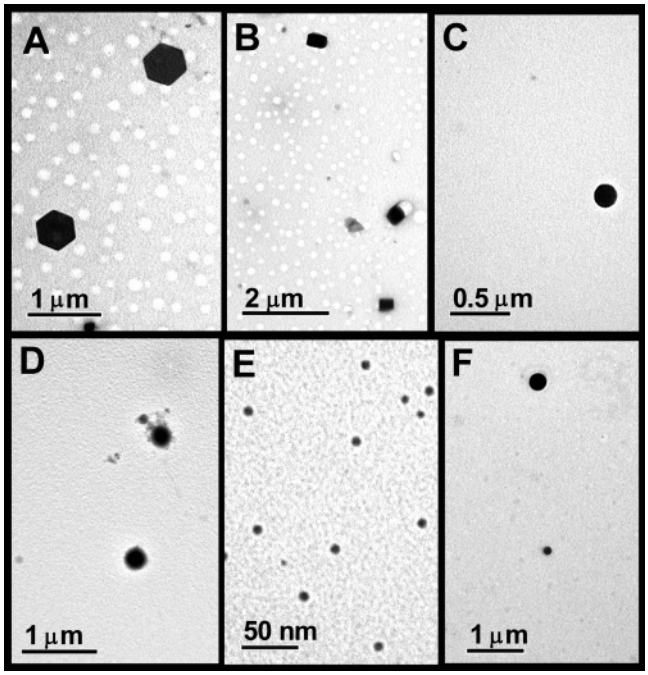

Figure 4. TEM images of particles formed with Pdase 017 and (A−C) $[Pt_2(DBA)_3]$, (D) $[Pd(PPh_3)_4]$, (E) $[Pt(PPh_3)_4]$, and (F) $[Ni(PPh_3)_4]$.

When $[Pt_2(DBA)_3]$ was incubated with Pdase 34, hexagonal and cubic particles were the major shapes observed. Changing the ligand to PPh_3, however, again resulted in loss of shape control by the RNA for all metals examined. Taken together, these results imply a correlation between Pd or Pt ligand−metal bond strength and shape control of the RNA Pdase to create hexagonal particles. The weaker σ donor ligands DBA as compared to triphenylphosphine gave consistently higher yields of hexagonal particles for both Pd and Pt.

Discussion

The goals of this study were to better understand the effects of RNA primary sequence and metal precursor on RNA-mediated growth of metal particles. Perhaps the most surprising result was the discovery of a sequence (Pdase 34) that codes for Pd cubes rather than hexagonal platelets, the exclusive product of all other sequences studied to date. Though sharing the same 5′- and 3′-fixed sequence regions, Pdases 17 and 34 are individually unique by way of their evolved sequence regions and do not share a common conserved region (Figure 1). While the deeper fundamental structural origins for the observed differences are not known at this time, the implication of the result is that a single in vitro selection can result in multiple catalytic RNA sequences, which, depending on their structure, assemble discrete crystal shapes with a high degree of specificity.

The results obtained from Pdase 17 sequence truncates 1 and 2 provide information regarding the length of RNA template required to mediate the formation of hexagonal Pd particles. It appears that the four nucleotide bases between the conserved region and the fixed 3′-region, or a portion thereof, are somehow critical to the structure of the Pdase and its ability to direct particle shape with a high degree of specificity. We hypothesize that these portions of the Pdases are strong determinants of secondary structure; removing them likely disrupts a critical folding motif necessary for proper interaction with the precursor complex or juxtaposition of the growing particle with incoming Pd^0 fragments. The precise length of the fixed 3′-region that is necessary to exclusively form hexagons has yet to be determined.

Replacing the pyridyl-modified uridine with native uridine resulted in complete loss of RNA catalytic activity. This loss of activity could be a combination of changes in 3D structure or the absence of an essential functional group at the catalytic site. The metal−ligand dependence on both the rate of particle formation as well as the specifity of crystal shape might suggest that ligand elimination is an important aspect of the particle growth mechanism. It remains to be determined if the pyridyl modification plays an active role in either the associative or dissociative elimination of DBA ligands from the Pd precursor organometallic complex.

In addition to sequence-dependent shape control, it is apparent that formation of Pd particles is highly dependent upon the ligand of the precursor complex. Changing the metal from Pd to Pt, while keeping the DBA ligand constant, did not compromise the ability of Pdases 17 or 34 to form particles, but did result in a slight decrease in shape specificity with a wider range of products being observed (cubes, hexagons, and spheres). However, in the case of Pdase 17, changing the ligand from DBA to the more tightly bound ligand triphenylphosphine was detrimental to both the number and specificity of particle shapes that could be found by TEM.

Taken together, the results show that the full-length Pdases 17 and 34 evolved through the course of the in vitro selection to recognize a specific metal−ligand set, $[Pd_2(DBA)_3]$. Changes in sequence length, base composition, metal, and ligand all affect the ability of these RNA sequences to mediate the formation of metal particles. These results suggest highly structured catalytic sites in these Pdases that can discriminate between metal precursors and their associated ligands. Interestingly, for the Pd and Pt DBA complexes, shape specifity was largely preserved favoring the formation of previously unknown hexagonal Pt particle plates. Consistent with increased metal−ligand bond strength and Pdase 17 playing an active role in elimination of ligand, the Pt particles were significantly smaller than the Pd particles under the same incubation conditions.

Conclusions

Biomimetic strategies are useful alternatives for exploring how to control particle growth. In contrast to controlling particle size and shape with surfactant or polymer capping reagents typically used in large excess, biopolymers such as RNA can form highly structured active sites that can dictate the formation of different shape particles from the same input metal precursors under identical conditions. Many unanswered questions remain regarding how the Pdase RNA structures accomplish the assembly of relatively large particles rapidly with a high degree of shape control. Clearly we now know that the ligand bound to the metal is more important to the control of shape in this process than an isoelectronic metal from the same row of the periodic table. However, metal−ligand bond strengths cannot be ignored as they undoubtedly influence the rate of particle formation. Using in vitro selection to explore the catalytic landscape of RNA for the assembly of inorganic materials has revealed new possibilities for the creation of previously

unknown Pd and Pt particle shapes, and there is much to learn about this process.

Experimental Section

Reagents. All reagents were used without further purification. Tris(dibenzylideneacetone) dipalladium(0) was purchased from Alfa Aesar. Tetrakis(triphenylphosphine) palladium(0) and tetrakis(triphenylphosphine) platinum(0) were purchased from Strem. Tetrakis(triphenylphosphine) nickel(0) was purchased from Acros. Milli-Q water was treated with diethylpyrocarbonate (depc) prior to use to ensure nuclease- and protease-free water.

Generation of RNA Isolates. RNA isolates were prepared by transcription of dsDNA templates. 4% (w/v) PEG 8000, 40 mM Tris-HCl, pH 8.0, 12 mM $MgCl_2$, 5 mM dithiothreitol (DTT), 1 mM spermidine HCl, 0.002% Triton X-100, 0.2 mM each of ATP, CTP, GTP, and 5-(4-pyridylmethyl)-uridine-5′-triphosphate, 125 nM T7 RNA polymerase (Promega), 0.8 units/μL RNase inhibitor (Promega) were incubated to yield 5-(4-pyridylmethyl)-uridine modified RNA transcripts (87-mer): 5′-GGGAGACAAGAATAAACGCTCGG-40 nucleotides-TTCGACAGGAGGCTCACAACAGGC-3′.

Formation of Metal Nanoparticles. RNA sequences (1 μM) were incubated in the presence of the metal complex precursor (400 μM). The following metal precursors were investigated: tris(dibenzylideneacetone) dipalladium(0) ($[Pd_2(DBA)_3]$), tris(dibenzylideneacetone) diplatinum(0) ($[Pt_2(DBA)_3]$), tetrakis(triphenylphosphine) palladium(0) ($[Pd(PPh_3)_4]$), tetrakis(triphenylphosphine) platinum(0) ($[Pt(PPh_3)_4]$), and tetrakis(triphenylphosphine) nickel(0) ($[Ni(PPh_3)_4]$). The organometallic complexes were each dissolved in freshly distilled (K, benzophenone) THF to give a concentration of 8 mM. This THF solution was then added to water (pH 7), giving an aqueous solution of 5% THF and 400 μM organometallic precursor. The incubations were performed in aqueous solution for 2 h at ambient temperature. Size-exclusion membranes (Microcon 100, 100-kD cutoff) were used to separate the RNA-bound metal particles from free RNA and unincorporated metal precursor. The reaction mixture was first concentrated onto the membranes by centrifugation and washed four times with buffer containing NaCl (1 mM), KCl (1 mM), $CaCl_2$ (1 mM), $MgCl_2$ (1 mM), and Na_3PO_4 (1 mM, pH 7.2) followed by two water (pH 7) washes to remove excess salts. The RNA-bound metal particles were recovered from the membrane by being resuspended in water.

Electron Microscopy. TEM was performed at the University of North Carolina School of Dentistry using a Philips CM12 transmission electron microscope operating at 100 kV accelerating voltage. To prepare samples for analysis, an aqueous solution of RNA-bound metal particles was drop-cast onto carbon-coated copper TEM grids (Formvar support, 300 mesh, Ted Pella). Bright-field images were captured digitally with Digital Micrograph using a Gatan 780 DualVison camera.

Acknowledgment. We thank the W. M. Keck Foundation and the National Science Foundation (CHE 0414527) for partial support of this work. We also thank Dr. Wallace Ambrose at the University of North Carolina for help with electron microscopy.

JA055039O